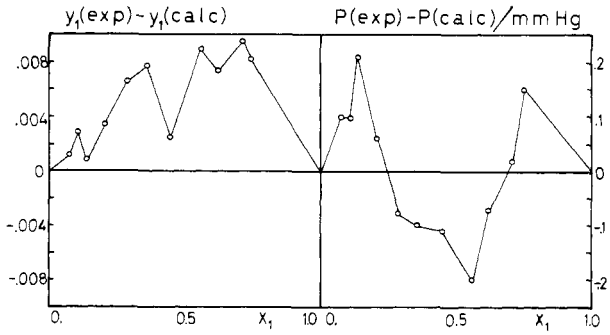

Figure 1. Deviations between experimental and calculated values of y_1 and P for ethyl acetate (1)–acetic acid (2) at 338 K.

with the UNIQUAC model were almost identical with the results with the Margules equations. An example is shown in Table VII for the system ethyl proprionate (1)–propionic acid (2) at 368 K. The slight differences between the root mean squared deviations for UNIQUAC in Tables VI and VII are due to small differences in the programs by Kemény et al. (*10*) and Prausnitz et al. (*12*).

Conclusion

The mean deviations between the experimental and calculated values of P, T, x, and y are comparable to the experimental uncertainties. All four data sets may therefore be considered to be thermodynamically consistent and the data sets may be included in the data base of reliable VLE data for UNIFAC parameter estimations.

Acknowledgment

We are most grateful to Claus Christensen and Ole Persson for all their assistance with the laboratory work.

Glossary

a_{12}, a_{21}	UNIQUAC parameters in Kelvin
A, B, C	constants in the Antoine equation
P	pressure in mmHg
P_i^0	vapor pressure in mmHg of component i
q_i	surface area parameter of component i
r_i	volume parameter of component i
t	temperature °C
T	temperature in Kelvin
x_i	liquid-phase mole fraction of component i
y_i	vapor-phase mole fraction of component i
ϕ_i	fugacity coefficient of component i in mixture
ϕ_i^0	fugacity coefficient of pure component i
γ_i	activity coefficient

Literature Cited

(1) Fredenslund, Aa.; Gmehling, J.; Rasmussen, P. "Vapor–Liquid Equilibria Using UNIFAC"; Elsevier: Amsterdam, 1977.
(2) Gmehling, J.; Rasmussen, P.; Fredenslund, Aa. *Ind. Eng. Chem. Process Des. Dev.* **1982**, *21*, 118.
(3) Andreeva, N. G.; Komarova, L. F.; Garber, Yu. N.; Anikeev, V. S. *Zh. Prikl. Khim. (Leningrad)* **1976**, *49*, 1161.
(4) Balashov, M. I.; Serafimov, L. A. *Khim. Khim. Tekhnol.* **1966**, *9*, 885.
(5) Garner, F. H.; Ellis, S. R. M.; Pearce, C. J. *Chem. Eng. Sci.* **1954**, *3*, 48.
(6) Hirata, M.; Hirose, Y. *Kagaku Kogaku* **1966**, *30*, 121.
(7) Othmer, D. *Ind. Eng. Chem.* **1943**, *35* 614.
(8) Schmidt, J. *J. Russ. Phys.-Chem. Soc.* **1930**, *62*, 1847.
(9) Dvorak, K.; Boublik, T. *Collect. Czech. Chem. Commun.* **1963**, *28*, 1249.
(10) Kemény, S.; Skjold-Jørgensen, S.; Manczinger, J.; Tóth, K. *AIChE J.* **1982**, *28*, 20.
(11) Abrams, D. S.; Prausnitz, J. M. *AIChE J.* **1975**, *21*, 116.
(12) Prausnitz, J.; Anderson, T.; Grens, E.; Eckert, C.; Hsieh, R.; O'Connell, J. "Computer Calculations for Multicomponent Vapor–Liquid and Liquid–Liquid Equilibra"; Prentice-Hall: Englewood Cliffs, NJ, 1980.

Received for review December 31, 1981. Accepted June 8, 1982. We thank STVF (Statens Teknisk Videnskabelige Forskningsråd) and NATO (Grant No. 1751) for financial support of this work, and Junta Nacional De Investigacão Cientifica e Tecnologica (Comissão Invotan)—Lisboa for a grant to E.A.M.

Phase Equilibria in the H_2/C_2H_6 System at Temperatures from 92.5 to 280.1 K and Pressures to 560 MPa

Andreas Heintz[†] and William B. Streett*

School of Chemical Engineering, Cornell University, Ithaca, New York 14853

Experimental data for liquid–vapor phase compositions of H_2/C_2H_6 are reported for 19 temperatures in the range 92.5–280.1 K and pressures up to 560 MPa. The data have been obtained by using a vapor-recirculating apparatus. The entire region of liquid–vapor coexistence has been explored for the first time. The mixture critical line and the pressure–temperature trace of the three-phase line solid–liquid–vapor have been located. These lines intersect at 138 K and 725 MPa to form an upper critical end point. Results obtained up to 52 MPa have been compared to published data.

Introduction

The study of the phase behavior of H_2/C_2H_6 presented in this paper continues in the research work on H_2/X systems reported in previous papers (*1–5*); these studies are designed to provide accurate data for design purposes and to explore patterns of phase behavior in H_2/X systems at high pressures. H_2 and ethane are both important components in industrial processes. The separation of H_2 from gases like ethane and other lower hydrocarbons requires the knowledge of the phase diagram of the binary mixtures. Optimal conditions for separation processes are often found at higher pressures. systematic and accurate data covering wide ranges of temperature and pressures are also important for testing theoretical methods of phase equilibrium prediction.

Data available in the literature for H_2/C_2H_6 are limited to 52 MPa (*6*, *7*) and cover only a small portion of the entire liquid-

[†] Visiting Fellow 1981/82. Permanent address: Physikalisch-Chemisches Institut, University of Heidelberg, Im Neuenheimer Feld 253, D-6900 Heidelberg, West Germany.

0021-9568/82/1727-0465$01.25/0

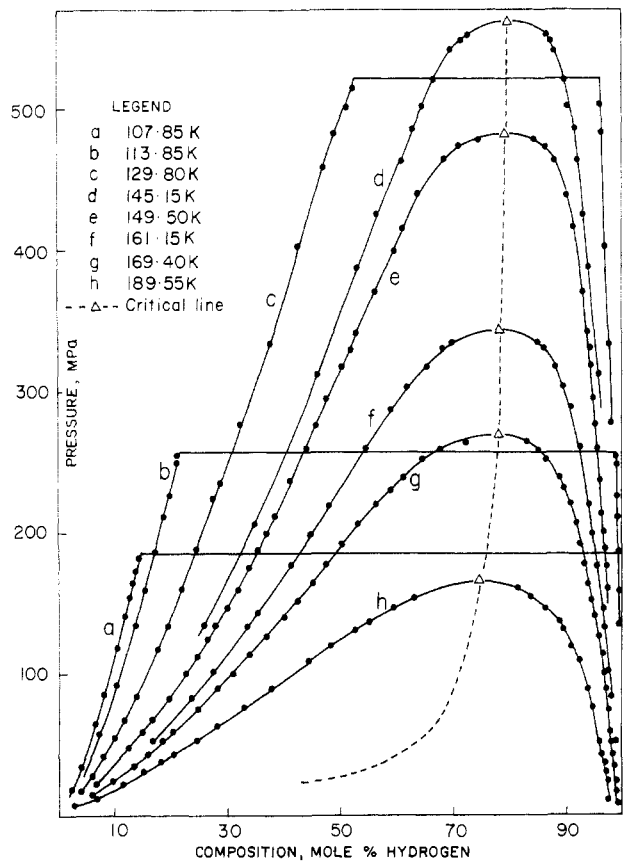

Figure 1. Experimental isotherms in the high-pressure region (to 500 MPa). The horizontal lines on isotherms a–c mark the pressures at which a solid phase is in equilibrium with the two fluid phases. The three-phase region appears as the line AB in Figure 3 and the shaded surface AFBEA in Figure 4.

vapor region. The purpose of this paper is to present a complete picture of the fluid phase behavior of H_2/C_2H_6 mixtures. The apparatus and method used in our study is essentially the same as described by Streett and Calado (*1*). The apparatus employs a vapor-recirculating equilibrium system using a magnetic pump. It has been modified by replacing the magnetic pump and the equilibrium cell used in earlier studies of H_2/X systems to contain the higher pressures required for the study of H_2/C_2H_6. Temperature is controlled by regulating the vapor pressure of a bath of boiling liquid. N_2, CH_4, CF_4, C_2H_6, and Freon 22 have been used as refrigerants to cover the temperature range between 92.5 and 280.1 K. Pressures are measured by an Autoclave Model DPS digital pressure gage up to 130 MPa and a Manganin resistance pressure gage for pressures above 130 MPa. The gages have been calibrated in this laboratory against a Ruska dead-weight gage. Compositions of the phases in equilibrium are measured by a calibrated thermal conductivity cell. The H_2 used in this work was Air Products ultrahigh purity (>99.999%) and the ethane was supplied by Matheson with purity of 99.9% (principal impurity H_2).

Results

Vapor–liquid compositions for H_2/C_2H_6 have been measured at 19 temperatures from 92.5 to 280.1 K and pressures up to 560 MPa. Results are recorded in Table I. X_1 and Y_1 are the mole fractions of H_2 in the liquid phase and the gaseous phase, respectively. Temperatures recorded in Table I are accurate to within ±0.02 K and pressures to ±0.5% of the measured values. Uncertainties in the phase compositions, due mainly to errors associated with sampling, are estimated to be ±0.003

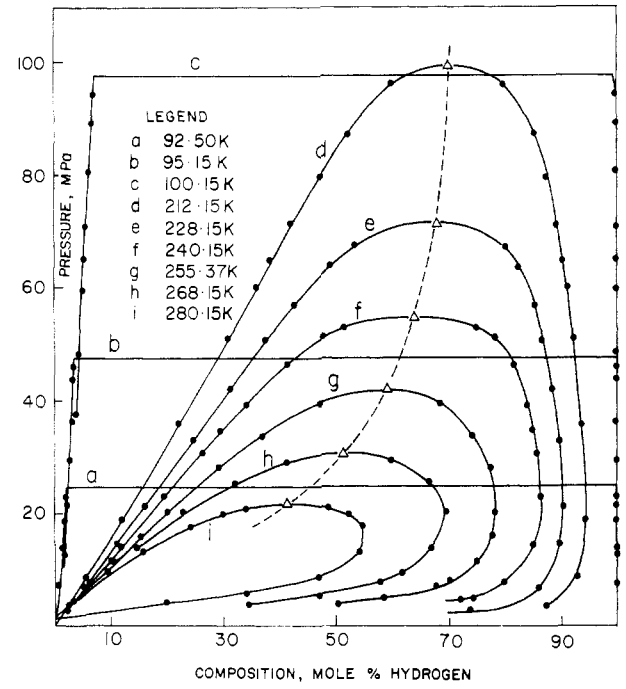

Figure 2. Experimental isotherms in the pressure range to 100 MPa (see caption to Figure 1).

in the mole fraction, although this may be as large as ±0.01 near the critical region.

The data obtained are plotted in $P-X$ diagrams. Figure 1 shows isotherms in which the maximum pressure exceeds 100 MPa. Figure 2 is a $P-X$ diagram in an expanded scale to show isotherms in the region of lower pressures. To avoid confusion not all isotherms and data points listed in Table I are shown in Figures 1 and 2. For isotherms above 130 K measurements could be made up to the critical region. Critical points have been obtained by extrapolating the liquid and vapor lines to contact at the top of each loop. The triangles in Figures 1 and 2 indicate the mixture critical points. At isotherms below 130 K the three-phase line solid–liquid–gas was encountered before a critical point could be reached. The horizontal lines in Figures 1 and 2 mark the pressures at which the solid phase is formed. The presence of a solid phase was detected by observing the pressures at which the recirculation of the vapor was abruptly halted by freezing in the lines of the apparatus. The composition of the solid phase cannot be determined by our experimental method. The solid phase, however, is likely to consist of nearly pure ethane in which only traces of hydrogen are dissolved.

The mixture critical line, the locus of points at which coexisting liquid and gas phases become identical, and the three-phase line, the freezing pressure of the mixture as a function of temperature, are shown in a $P-T$ diagram in Figure 3. The curves intersect in an upper critical end point B at 138 K and 725 MPa. As the freezing pressures are accurate only to within ±0.3 MPa, the critical end point B obtained by extrapolation is estimated to be accurate to within ±0.3 K in temperature and only ±1.0 MPa in pressure, due to the steep slopes of both the three-phase line and the mixture critical line. The vapor–liquid coexistence region is bounded by three lines in Figure 3, namely, the vapor pressure curve AC of ethane, the mixture critical line CB, and the $P-T$ trace AB of the three-phase region. The properties of the mixture critical line are recorded in Table II. The pressure–temperature points of the three-phase region solid–liquid–gas are given in Table III. As in other H_2/X systems studied earlier (*1–5*) the triple-point temperature of the less volatile component is much higher than the critical temperature of H_2. Consequently, the mixture critical line, which

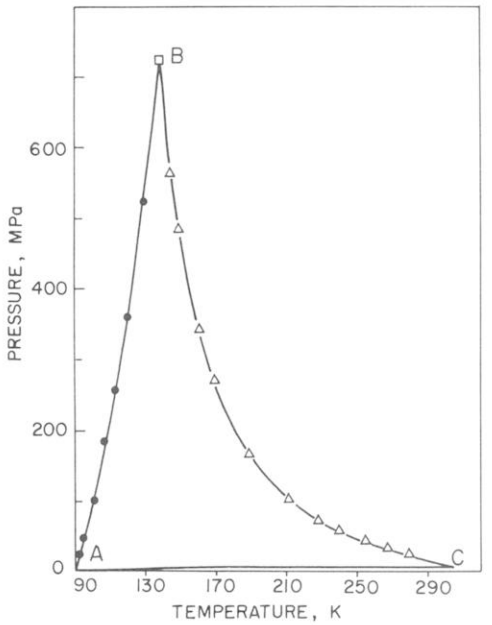

Figure 3. Pressure–temperature diagram showing the boundaries of the region of liquid–gas phase separation. AC is the vapor pressure curve of ethane, CB is the mixture critical line, and AB is the pressure–temperature trace of the three-phase region solid–liquid–gas.

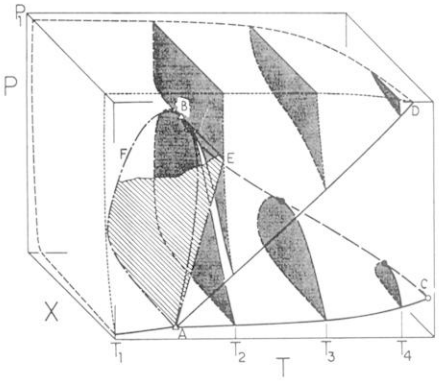

Figure 4. Schematic three-dimensional $P-T-X$ diagram for H_2/C_2H_6. The isotherm T_2 passes through the critical end point B. The lower (liquid–gas) and upper (solid–gas) branches of isotherm T_2 are tangent at this point. Isotherm T_1 and the upper branches of the remaining isotherms describe the region of solid–gas equilibrium, which has not been studied in this work. (see text for further discussion.)

emerges from the critical point C of ethane, does not extend continously to the critical point of hydrogen. Instead, it intersects the three-phase region, which emerges from the triple point of ethane, at the critical end point B. Unlike H_2/X systems studied so far the critical end point is located at much higher pressure in the H_2/C_2H_6 system. Compared to the H_2/CH_4 system, the lower analogue system in the H_2/hydrocarbon series, the mixture critical line CB of H_2/C_2H_6 starts at higher temperature, due to the higher critical temperature of C_2H_6. As the triple point of C_2H_6 (90.3 K) is almost the same as that of CH_4 (90.7 K), the mixture critical line meets the three-phase line in the H_2/C_2H_6 system at a much higher pressure than in the H_2/CH_4 system. No temperature minimum of the three-phase line exists for H_2/C_2H_6 as has been found for H_2/CH_4, H_2/Ar, and H_2/CO. The three-phase line is located closer to the melting curve of pure C_2H_6, indicating a lower depression of freezing temperature and less solubility of H_2 in liquid C_2H_6 than in N_2, CH_4, Ar, and CO.

From the equilibrium data obtained in our study a three-dimensional $P-T-X$ phase diagram can be constructed. This is shown in Figure 4 and illustrates qualitatively the features of the phase behavior of H_2/C_2H_6 which are similar to those of H_2/CO_2

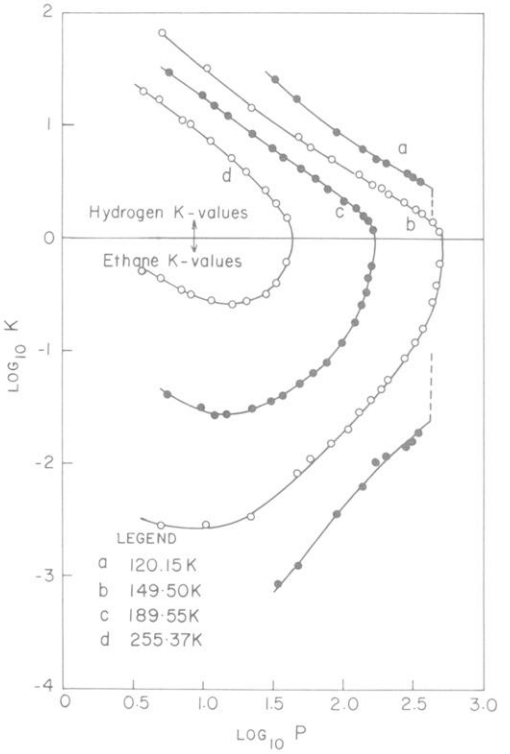

Figure 5. Plot of log K vs. log P, where $K \equiv Y_i/X_i$, the ratio of the mole fractions of component i in the vapor and liquid phases.

(*5*), although the liquid–vapor region extends to much higher pressures in the H_2/C_2H_6 system. Point A is the triple point of C_2H_6 and C its critical point, and AD is the melting curve of pure C_2H_6. AC and AD lie in the near $P-T$ face of the diagram. The dashed line CB is the mixture critical line, bounded at high pressure by the critical end point B. The region of coexistence of the three phases solid–liquid–gas is the surface AFBEA, partially shaded by parallel lines. In this region the three coexisting phases are represented by three lines: the vapor line AFB, the liquid line AB, and the solid line AE. The first two of these meet at the critical end point B, where the vapor and liquid phases become identical. At higher pressures only a single fluid phase exists in equilibrium with a solid phase at temperatures below the melting temperature of pure C_2H_6. Also at all $P-T$ states below temperatures bounded by the line AE a single fluid phase exists in equilibrium with a solid phase. According to the constraints imposed by the phase rule on a three-phase region, a system of two components and three phases has only one independent intensive property. If the temperature is chosen as the independent variable, for example, it follows that all remaining variables—pressure and phase compositions—are functions only of temperature. As a consequence the three lines AFB, AB, and AE in Figure 4, representing the three coexisting phases in $P-T-X$ space, lie in a ruled surface perpendicular to the $P-T$ plane and have common projection on that plane. This projection is the curve AB in Figure 3.

Internal consistency of the data is illustrated by plotting the logarithm of the equilibrium factor K vs. log P (Figure 5). Scattering in the data is generally somewhat higher for the ethane K values than for other solvents X in the H_2/X systems, due to the comparatively lower solubility of H_2 in ethane.

Comparison with Published Data

Comparison with data of other authors could be made only below 52 MPa. Williams and Katz (*6*) have published data in the temperature range 103–283 K and pressures up to 51.1 MPa. More recently Hiza, Heck, and Kidnay presented data on

Table I. Liquid-Vapor Phase Composition for H_2/C_2H_6

P, MPa	X_1	Y_1	P, MPa	X_1	Y_1
		T = 92.50 K			
7.58	0.0072	1.0000	18.96	0.0181	1.0000
13.92	0.0142	1.0000	23.37	0.0209	1.0000
		T = 95.15 K			
12.96	0.0142	1.0000	36.60	0.0305	1.0000
15.23	0.0161	1.0000	44.10	0.0349	1.0000
21.95	0.0213	1.0000	46.20	0.0354	1.0000
29.57	0.0263	1.0000			
		T = 100.15 K			
11.44	0.0152	1.0000	65.15	0.0523	0.9993
21.05	0.0242	1.0000	71.21	0.0571	0.9994
37.04	0.0357	1.0000	80.08	0.0621	0.9992
48.55	0.0431	0.9999	89.63	0.0663	0.9992
59.66	0.0503	0.9993	93.91	0.0704	0.9992
		T = 107.85 K			
8.17	0.0124	0.9996	142.93	0.1201	0.9955
19.50	0.0267	0.9995	155.68	0.1278	0.9941
35.58	0.0413	0.9995	163.67	0.1327	0.9929
65.52	0.0678	0.9993	165.82	0.1340	0.9932
86.22	0.0820	0.9969	173.40	0.1385	
118.55	0.1039	0.9960	182.78	0.1468	
		T = 113.85 K			
59.06	0.0725		212.15	0.1873	0.9920
93.91	0.1038		227.39	0.1970	0.9913
135.36	0.1370	0.9955	251.23	0.2110	0.9904
159.82	0.1547	0.9945	255.79	0.2146	0.9902
187.39	0.1704	0.9924			
		T = 120.15 K			
47.75	0.0730	0.9991	285.71	0.2650	0.9895
90.73	0.1172	0.9968	314.40	0.2822	0.9881
140.58	0.1635	0.9948	329.29	0.2925	0.9874
172.85	0.1888	0.9915	337.84	0.2970	0.9868
204.50	0.2126	0.9914	345.42	0.3013	0.9868
243.45	0.2370		351.63	0.3040	0.9859
		T = 129.80 K			
7.50	0.0173	0.9983	189.19	0.2472	0.9884
17.75	0.0402	0.9978	225.87	0.2784	0.9873
28.43	0.0602	0.9976	236.49	0.2910	0.9833
42.42	0.0822	0.9963	278.46	0.3266	0.9818
54.69	0.1002	0.9956	334.40	0.3767	0.9760
67.48	0.1182	0.9946	404.58	0.4266	0.9716
69.15	0.1193	0.9935	460.01	0.4765	
84.42	0.1401	0.9899	461.94	0.4762	0.9685
118.59	0.1786	0.9896	484.83	0.4865	0.9665
134.86	0.1951	0.9890	503.31	0.5166	0.9642
136.24	0.1959	0.9894	514.60	0.5281	
161.06	0.2213	0.9890			
		T = 135.15 K			
87.80	0.1595	0.9907	386.10	0.4675	0.9652
134.55	0.2169	0.9884	526.75	0.6021	0.9524
272.86	0.3630	0.9762	559.50	0.6392	0.9456
		T = 145.15 K			
135.39	0.2616	0.9830	487.86	0.6288	0.9158
207.46	0.3515	0.9740	504.34	0.6460	0.9039
313.43	0.4606	0.9573	522.61	0.6678	0.8970
389.20	0.5336	0.9422	544.06	0.6979	0.8810
427.19	0.5673	0.9309	551.23	0.7178	0.8758
465.40	0.6111	0.9226	555.02	0.7256	0.8691
		T = 149.50 K			
5.14	0.0147	0.9973	209.18	0.3816	0.9659
11.23	0.0365	0.9973	213.73	0.3858	0.9652
22.40	0.0685	0.9971	238.56	0.4145	0.9607
47.40	0.1264	0.9929	260.53	0.4403	0.9573
58.95	0.1531	0.9908	277.23	0.4578	0.9539
67.85	0.1683	0.9895	284.20	0.4669	0.9506
82.44	0.1972	0.9878	296.13	0.4772	0.9498
100.65	0.2280	0.9851	318.26	0.5049	0.9453
112.37	0.2470	0.9845	330.87	0.5213	0.9441
125.56	0.2675	0.9819	342.32	0.5275	0.9385
132.10	0.2763	0.9791	371.76	0.5632	0.9304
135.27	0.2809	0.9795	400.58	0.5999	
146.79	0.3007	0.9772	417.82	0.6128	0.9138
160.71	0.3201	0.9745	440.57	0.6402	0.9023
176.16	0.3404	0.9736	464.29	0.6872	0.8815
182.15	0.3456	0.9705	475.11	0.7112	0.8654
188.57	0.3550	0.9702	480.25	0.7483	0.8472
201.05	0.3708	0.9678	480.97	0.7519	
		T = 161.15 K			
53.94	0.1708	0.9857	261.58	0.5477	0.9251
83.60	0.2390	0.9797	285.37	0.5901	0.9087
101.92	0.2763	0.9760	304.05	0.6212	0.8959
134.26	0.3369	0.9684	318.33	0.6560	0.8818
144.32	0.3568	0.9657	331.91	0.6836	0.8598
178.50	0.4148	0.9556	332.94	0.6952	0.8583
199.53	0.4483	0.9483	335.43	0.7011	0.8512
220.69	0.4828	0.9427			
		T = 169.40 K			
6.74	0.0292	0.9893	141.75	0.4031	0.9513
14.35	0.0611	0.9899	152.37	0.4256	0.9441
24.50	0.0975	0.9877	165.47	0.4518	0.9393
35.11	0.1336	0.9851	178.99	0.4769	0.9312
43.28	0.1594	0.9830	192.57	0.5052	0.9251
52.26	0.1867	0.9815	204.84	0.5315	0.9191
59.44	0.2066	0.9782	207.39	0.5345	0.9181
60.08	0.2093	0.9782	218.97	0.5597	0.9115
75.63	0.2500	0.9767	221.46	0.5665	0.9083
89.55	0.2843	0.9711	232.49	0.5928	0.8978
102.17	0.3136	0.9678	240.07	0.6153	0.8906
114.33	0.3419	0.9631	247.59	0.6322	0.8798
126.76	0.3678	0.9582	253.73	0.6462	0.8664
130.19	0.3759	0.9562	260.48	0.6771	0.8514
132.03	0.3777	0.9549	265.72	0.7250	0.8341
135.18	0.3852	0.9548			
		T = 189.55 K			
5.75	0.0325	0.9605	63.91	0.2864	0.9550
9.86	0.0526	0.9702	66.51	0.2954	0.9534
12.76	0.0680	0.9749	77.46	0.3334	0.9475
15.20	0.0789	0.9740	90.37	0.3795	0.9388
22.71	0.1162	0.9736	100.64	0.4144	0.9309
27.85	0.1353	0.9718	110.51	0.4467	0.9223
31.38	0.1531	0.9706	112.04	0.4519	0.9194
34.91	0.1702	0.9697	121.75	0.4864	0.9082
37.94	0.1840	0.9682	131.40	0.5182	0.8946
43.32	0.2053	0.9640	132.52	0.5276	0.8948
50.16	0.2323	0.9602	138.04	0.5519	0.8828
53.70	0.2472	0.9611	148.37	0.5908	0.8631
55.91	0.2532	0.9595	155.88	0.6323	0.8360
63.60	0.2840	0.9550	161.61	0.6778	0.8155
		T = 212.15 K			
3.94	0.0263	0.8752	65.01	0.3831	0.9036
8.77	0.0565	0.9290	71.50	0.4235	0.8938
19.13	0.1224	0.9432	79.91	0.4753	0.8751
36.02	0.2235	0.9368	87.42	0.5227	0.8529
51.47	0.3102	0.9223	96.33	0.6006	0.7989
60.20	0.3603	0.9117			
		T = 228.15 K			
3.18	0.0219	0.7389	42.33	0.3141	0.8838
7.06	0.0535	0.8621	50.70	0.3754	0.8667
14.79	0.1120	0.8964	57.08	0.4272	0.8546
21.45	0.1621	0.9055	63.81	0.4922	0.8233
33.20	0.2467	0.8970	67.57	0.5358	0.8005
		T = 240.15 K			
4.79	0.0341	0.7248	34.74	0.2967	0.8489
4.92	0.0344	0.7445	39.47	0.3421	0.8413
7.89	0.0632	0.7998	46.57	0.4135	0.8158
14.40	0.1192	0.8472	51.55	0.4760	0.7807
23.17	0.1969	0.8651	53.18	0.5149	0.7514
30.98	0.2655	0.8568			
		T = 255.37 K			
3.80	0.0258	0.5042	16.05	0.1551	0.7752
4.93	0.0347	0.5833	20.49	0.2027	0.7794
7.14	0.0610	0.6737	28.37	0.2917	0.7741
8.22	0.0696	0.6998	33.97	0.3671	0.7420
11.56	0.1060	0.7473	39.59	0.4731	0.6855

Table I (*Continued*)

P, MPa	X_1	Y_1	P, MPa	X_1	Y_1	P, MPa	X_1	Y_1	P, MPa	X_1	Y_1
		$T = 268.15$ K						$T = 280.15$ K			
3.90	0.0234	0.3443	13.95	0.1497	0.6673	4.09	0.0192	0.2001	17.71	0.2456	0.5480
5.44	0.0394	0.4684	20.35	0.2306	0.6960	5.85	0.0448	0.3382	19.88	0.3018	0.5216
7.86	0.0711	0.5769	25.61	0.3214	0.6669	8.67	0.0855	0.4697	20.86	0.3385	0.4871
9.39	0.0896	0.6144	29.38	0.4140	0.5988	13.28	0.1597	0.5425			

Table II. H_2/C_2H_6 Critical Properties

T, K	P, MPa	H_2, mol %	T, K	P, MPa	H_2, mol %
145.15	562.5	79.8	228.15	71.5	69.0
149.50	483.0	79.3	240.15	55.0	64.3
161.15	341.5	78.3	255.37	42.0	59.5
169.40	268.5	77.5	268.15	30.5	51.5
189.55	164.5	74.8	280.15	21.5	41.8
212.15	100.0	70.5			

Table III. Pressure-Temperature Points in the Three-Phase Region Solid-Liquid-Vapor

T, K	P, MPa	T, K	P, MPa
92.50	24.6	113.85	257.5
95.15	47.5	120.15	358.5
100.15	98.0	129.80	523.0
107.85	184.5		

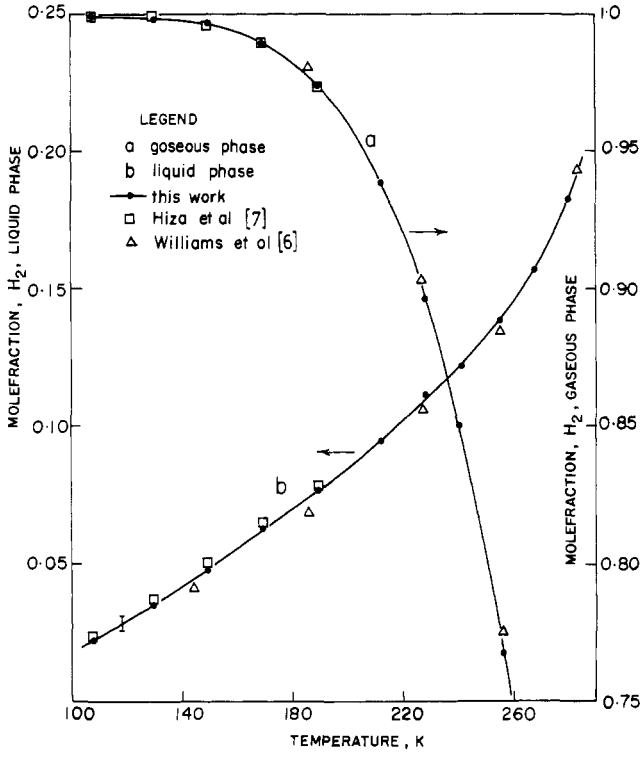

Figure 6. comparison with published data at 14.6 MPa.

the liquid–gas and solid–gas phase equilibrium from 80.0 to 189.5 K and pressures up to 14.8 MPa (*7*). Comparisons with present data are shown in Figures 6 and 7. Our results in Figures 6 and 7 are interpolated from the direct experimental data. The data of Williams and Katz as well as those of Hiza et al. show good agreement with our results and lie within the error limits estimated for our experimental method.

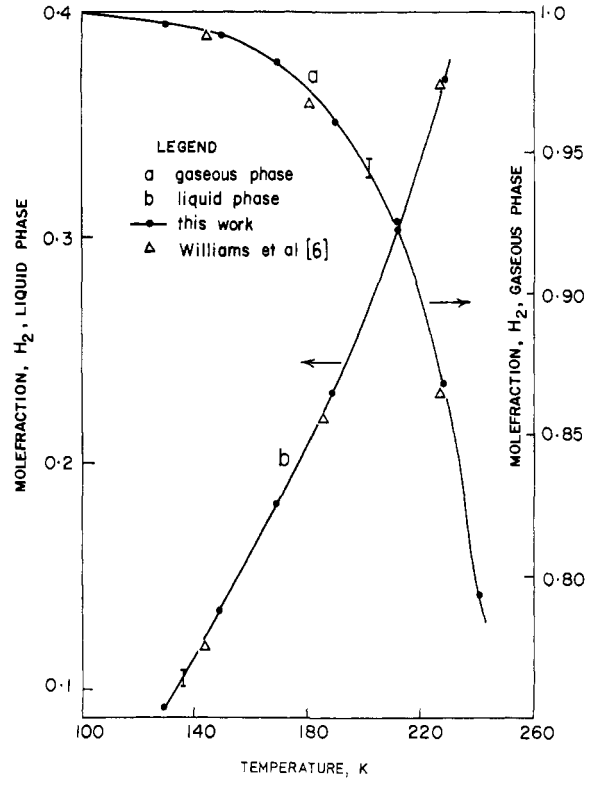

Figure 7. Comparison with published data at 50.0 MPa.

Comparison with Equation of State and Theoretical Predictions

Calculations are now being carried out to compare these experimental results, as well as earlier measurements for other H_2/X systems, with the predictions of cubic equations such as the Peng–Robinson and Redlich–Kwong equations, and with statistical mechanical perturbation theory (*8*). The results of these comparisons will be published separately.

Literature Cited

(1) Streett, W. B.; Calado J. C. G. *J. Chem. Thermodyn.* **1978**, *10*, 1089–100.
(2) Calado, J. C. G.; Streett, W. B. *Fluid Phase Equilib.* **1979**, *2*, 275–82.
(3) Tsang, C. Y.; Clancy, P.; Calado, J. C. G.; Streett, W. B. *Chem. Eng. Commun.* **1980**, *6*, 365–83.
(4) Tsang, C. Y.; Streett, W. B. *Fluid Phase Equilib.* **1981**, *6*, 261–73.
(5) Tsang, C. Y.; Streett, W. B. *Chem. Eng. Sci.* **1981**, *36*, 993–1000.
(6) Williams, R. B.; Katz, D. L. *Ind. Eng. Chem.* **1954**, *46*, 2512–20.
(7) Hiza, M. J.; Heck, C. K.; Kidnay, A. J. *Adv. Cryog. Eng.* **1968**, *13*, 343–56.
(8) Clancy, P.; Gubbins, K. E. *Mol. Phys.* **1981**, *44*, 581–95.

Received for review April 22, 1982. Accepted July 23, 1982. Acknowledgment is made to the donors of the Petroleum Research Fund, administered by the American Chemical Society, for partial support of this work, and to the National Science Foundation and NATO, for additional support. A.H. acknowledges a generous fellowship from the Deutsche Forschungsgemeinschaft.